Regular Article

PHYSICAL CHEMISTRY RESEARCH
Published by the
Iranian Chemical Society
www.physchemres.org
info@physchemres.org

***Phys. Chem. Res.**, Vol. 1, No. 2, 142-151, December 2013.*

A Theoretical Survey on Strength and Characteristics of F···F, Br···O and Br···Br Interactions in Solid Phase

M.D. Esrafili[a,*] and M. Solimannejad[b,*]

[a]*Laboratory of Theoretical Chemistry, Department of Chemistry, University of Maragheh, Maragheh 5513864596, Iran*
[b]*Quantum Chemistry Group, Department of Chemistry, Faculty of Sciences, Arak University, Arak 38156-8-8349, Iran*

(Received 18 June 2013, Accepted 23 August 2013)

A quantum chemical investigation was carried out to study the properties of intermolecular F···F, Br···Br and Br···O interactions in crystalline 1-bromo-2,3,5,6-tetrafluoro-nitrobenzene (BFNB). This system was selected to mimic the halogen-halogen as well as halogen bonding interactions found within crystal structures and biological systems. We found that fluorine atoms have weak positive electrostatic potentials ($V_{S,max} \approx +1$ kcal mol^{-1}) which could be responsible for their weak electrophilic behavior. According to quantum theory of atoms in molecules, the values of electron density at the F···F critical points are calculated to be in a range of 0.004-0.006 au, whereas the values of $\nabla^2\rho_{BCP}$ are all positive, ranging from 0.023-0.031 au. This indicates that all F···F interactions in crystalline BFNB, are weak and basically electrostatic in nature. The nature of intermolecular interactions is analyzed using energy decomposition analysis (EDA). Our results indicate that, for those nuclei participating in intermolecular interactions, nuclear magnetic resonance parameters exhibit considerable changes on going from the isolated gas phase molecule model to crystalline BFNB. Of course, the magnitude of these changes at each nucleus depends directly on its amount of contribution to the interactions.

Keywords: Halogen bonds, Electrostatic potential, DFT, NMR, QTAIM

INTRODUCTION

Non-covalent interactions play key roles in many chemical phenomena, such as supramolecular chemistry, molecular recognition, bioligical structure, and molecular packing in crystals [1-5]. The most common of these are hydrogen bonding interactions, frequently defined as an X-H···Y interaction, where X and Y are electronegative elements and Y possesses one or more lone electron pairs. However, one can also mention so-called unconventional hydrogen bonding such as C-H···Y, X-H···C, X-H···π-electrons interactions [6]. A halogen bond can be described in general by R-X···B interaction, in which X is an electrophilic halogen atom (typically chlorine, bromine, or iodine) and B is any negative site, including Lewis bases, π regions of aromatics or molecules containing double bonds, and anions [7,8]. The R-X···B angle is typically close to 180°, which suggests that the halogen bond is a highly directional interaction. Halogen bonds share numerous chemical and physical properties with the hydrogen bonds [9-13] and it was exciting to see that halogen bonding prevailed over hydrogen bonding in a competitive recognition process [14]. Although the halogen atom X as well as halogen bond electron donor B involved in a halogen bond may have a net negative charge, the stability of the halogen bond is explained by the existence of an electropositive crown at the top of the halogen atom directed toward the electron donor [15]. This positive potential that results from polarization of the halogen along its covalent bond extension, referred to as a "*σ*-hole" [16]. Extensive experimental results [17-19] and theoretical calculations [20-26] consistently reveal that the greater the polarizability and the lower the electronegativity of a halogen atom, the more positive is its *σ*-hole and the stronger is the halogen bond to which it gives rise.

Recently, several groups have reported weak closed-shell bonding interactions between halogens on the basis of

*Corresponding authors. E-mail: esrafili@maragheh.ac.ir; m-solimannejad@araku.ac.ir

the structural and energetics properties [27-30]. For halogens linked to carbons, certain distinct tendencies have been identified. It is proposed [31] that the halogen-halogen interactions are classified into two groups: type I and type II (Scheme 1). Tsirelson *et al.* [32] have described a closed-shell bonding interaction between chlorine atoms belonging to neighboring molecules in solid molecular chlorine crystals, the interaction that enables solid chlorine to exist in the crystalline form. As a result of a combination of extreme electronegativity and limited polarizability, the F atom is frequently deemed to not participate in X···X bonding. The electron density distribution around F is nearly spherical rather than anisotropic and, consequently, F is most likely to behave as a halogen bond acceptor. However, it has recently been shown that the fluorine atom has the capability of forming non-covalent X···X bonds and can also affect recognition and self assembly processes, but only under specific circumstances [33-35]. Bach and co-workers [36] have reported weak intermolecular F···F contacts in an electron density study of crystalline pentafluorobenzoic acid at 110 K using multipolar refinement. Matta *et al.* [37] employed electronic topology theory to analyze bond path linking to saturated fluorine atoms and concluded that the F···F bonding is shown to exhibit all the hallmarks of a closed-shell weak interaction. Alkorta and Elguero [38] found a correlation between the calculated electron density at the F···F bond critical point and the through-space fluorine-fluorine spin-spin coupling constant, J_{FF}, in six fluorinated organic compounds.

The aim of this study is to apply quantum chemical calculations and quantum theory of atoms in molecules (QTAIM) [39] to analyze the properties of F···F as well as Br···Br and Br···O interactions in solid 1-bromo-2,3,5,6-tetrafluoro-4-nitrobenzene (BFNB), see Fig. 1. In addition, the effects of such intermolecular interactions on the evaluated ^{19}F and ^{79}Br nucleal magnetic resonance parameters of BFNB are also studied. This system was selected to mimic the halogen-halogen as well as halogen bond interactions found within crystal structures and biological molecules. Such a theoretical study may provide some valuable information of the origin and strength of halogen-halogen and halogen bond interactions, which would be very important for the design and synthesis of new materials and effective drugs containing halogenated compounds.

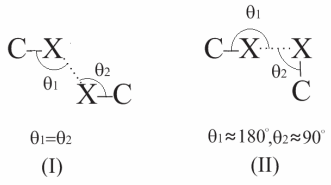

Scheme 1. Classification of halogen-halogen bonds

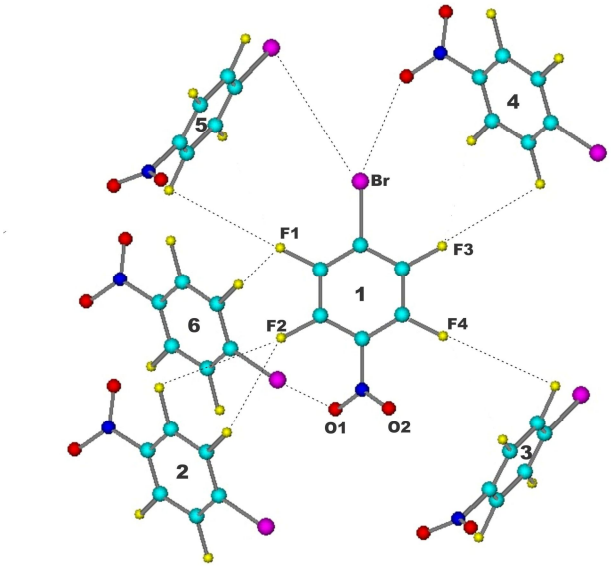

Fig. 1. Crystalline structure of BFNB. The dashed lines indicate intermolecular halogen bonds.

Computational Details

All calculations were performed using the GAMESS suite of programs [40]. For the density functional theory (DFT) calculations, B3LYP [41] and M06-2X [42] density functionals with 6-311++G** standard basis set were employed. B3LYP was selected, given its widespread use, and M06-2X was included because of its excellent performance on halogen bonding interactions [43]. Electrostatic potential for the BFNB molecule was computed using M06-2X/6-311++G** optimized geometry at the same level of theory. The model cluster used in this study was constructed from an experimental X-ray crystal structure for BFNB [44]. Interaction energies between BFNB monomers were computed at the M062X and MP2/6-311++G** levels of theory. The basis set superposition

error (BSSE) calculated with the counterpoise method [45] was used to correct the interaction energies. To gain a deeper insight into the characteristics of intermolecular interactions, interaction energies were decomposed using [46]:

$$E_{\text{int}} = E_{elst} + E_{exch-rep} + E_{pol} + E_{disp} \quad (1)$$

in which E_{elst} gives the electrostatic term describing the classical Coulumb interaction of the occupied orbitals of one monomer with those of another monomer, $E_{exch-rep}$ is the repulsive exchange-repulsion component resulting from the Pauli exclusion principle, E_{pol} and E_{disp} correspond to polarization and dispersion terms, respectively.

The absolute chemical shielding tensors at the sites of ^{19}F and ^{79}Br nuclei have been calculated at the B3LYP and M06-2X/6-311++G** levels of theory employing gauge-included atomic orbital, GIAO, approach [47]. The QTAIM [39] was applied to find bond critical points (BCPs) and to characterize them in terms of electron density, ρ_{BCP}, its Laplacian, $\nabla^2\rho_{BCP}$ and energy density quantities. All electron density analyses were performed by AIM2000 package [48].

RESULTS AND DISCUSSION

Geometries

Figure 2 indicates the evaluated surface electrostatic $V_S(r)$ map for the isolated BFNB moelcule. The figure shows the location of the various most positive ($V_{S,max}$) and most negative ($V_{S,min}$) potentials, all of which are located by the WFA code [49]. It is evident that the most negative electrostatic potential on the BFNB surface is associated with the oxygen atoms, $V_{S,min}$ = -28.5 (O1) and -27.0 (O2) kcal mol^{-1}. These are located in the NO_2 plane and can be attributed to the overlapping electronic densities of the oxygen unshared electrons pairs. The most striking feature of Fig. 2 is a positive electrostatic potential cap ($V_{S,max}$ = +43.1 kcal mol^{-1}) at the end region of the Br atom along the C-Br bond vector, which is surrounded by an electroneutral area and, next, a large electronegative domain. Such halogen positive region is referred as the "σ-holes", because it is centered on the C-X axis and is surrounded by negative electrostatic potential. This positive region can interact with an electronegative atom/group, thereby, giving rise to a highly directional interaction. It is also seen that fluorines have weak positive σ-holes ($V_{S,max} \approx$ +1 kcal mol^{-1}) which could be responsible for their weak electrophilic behavior. The same explanation has been also reported for the formation of other fluorine-centerd halogen bonded complexes [50].

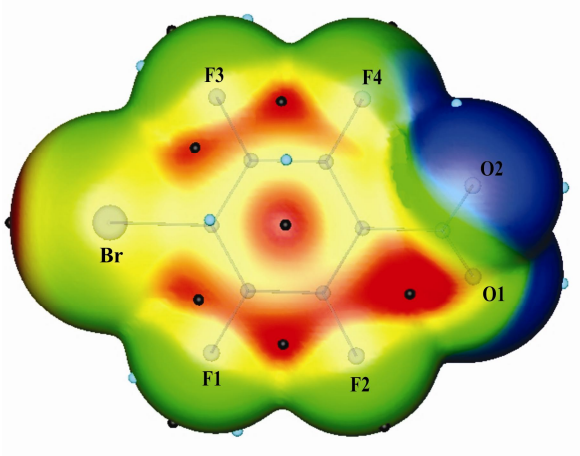

Fig. 2. Electrostatic potential mapped on the surface of BFNB molecular electron density (0.001 e au^{-3}). Color ranges, in kcal mol^{-1}, are: red > 26.1, yellow 7.9-26.1, green -10.0-7.9, blue < - 10.0. Black and blue circles are referred to surface maxima and minima, respectively.

As depicted earlier, the positive σ-holes in halogens are localized on the extensions of the covalent bonds in which they are involved. This explains the directionality which is a distinctive feature of halogen bond. The graphical illustration of the crystalline BFNB under consideration is depicted in Fig. 1. In addition to Br···O and Br···Br interactions, there are also F···F interactions that could be classed as type I or type II. The F···F intermolecular distances are in the range of 2.86-3.01 Å. Most of them are less than or in the vicinity of the sums of the van der Waals (vdW) radii of the respective atoms (2.94 Å) [51], which is consistent with these being weak noncovalent interactions. The Br···Br interaction is between the positive σ-hole on one bromine and the negative lateral side of another, illustrating the point discussed above. Inspection of results reveals that for the Br···Br interactions, the internuclear distances are slightly longer than the vdW radius sum of the two bromine

atoms (3.70 Å) [51], hence, they do not contribute significantly to the stabilization of the crystal packing. As evident from Fig. 1, the crystal structure of BFNB is characterized by the presence of short Br···O contacts, which are responsible for the formation of three-dimensional molecular network of BFNB. The Br···O distance is 3.15 Å, considerably shorter than the sum of van der Waals radii (3.37 Å).

It might be questioned whether F···F contacts are actually taking place in the solid BFNB, or are the observed fluorine short contacts simply the result of other noncovalent interactions. In a recent studty, Politzer and co-workers [52] analyzed the fluorine-centered halogen bonds properties in both the gasous and crystalline phases. Through statistical analyses of data from the Cambridge Structural Database (CSD), these authors demonstrated that the ability of fluorine to act as a halogen bond donor in solids is most likely to manifest itself when no stronger competing interactions determine the crystal packing, since these may preferentially dominate and prevent weak fluorine-centered halogen bonds from occurring. On the other hand, a positive σ-hole, and the resulting halogen bond, may be a structure-stabilizing factor only in systems where fluorine is close to strongly electron withdrawing groups. A recent search on the CSD by Barceló-Oliver *et al.* [33] yields 1658 compounds with F···F distances up to 3.0 Å of which only 34 (2.05%) compounds show F···F contacts of type II. Hence, the majority of F···F interactions present in crystalline phase can be classified as type I. This result is in disagreement with the proposal that only contacts of type II are stabilizing and that contacts of type I are caused only by close packing [35].

QTAIM Analysis

The QTAIM has been successfully applied in characterizing non-covalent interactions of different strengths in a wide variety of molecular systems [53-57]. According to QTAIM, properties of BCP serve to summarize the nature of the interaction between two atoms as covalent interactions (also known as "open-shell" interactions) or closed-shell interactions (*e.g.*, ionic, van der Waals, or HBs). The value of ρ at a BCP, ρ_{BCP}, gives a loose indication of bond strength [39]. However, a clear distinction between the closed-shell and covalent type of

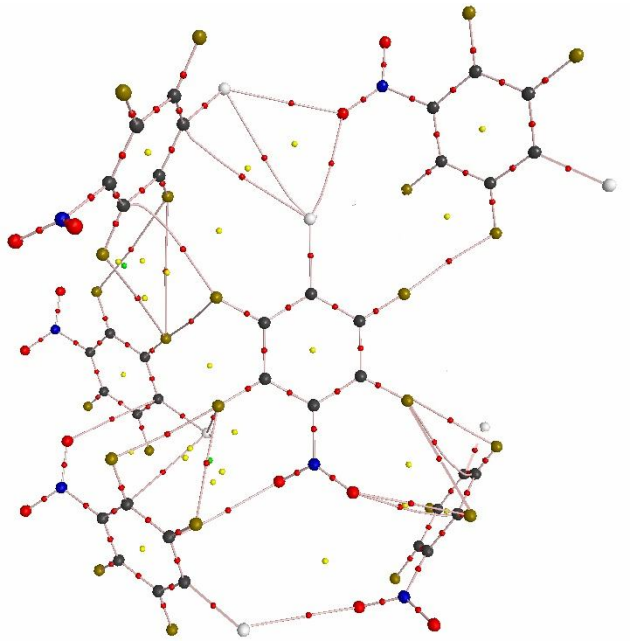

Fig. 3. Molecular graph of crystalline BFNB, *solid lines* indicate bond paths and *large circles* correspond to attractors, *small red* ones to BCPs.

interaction is impossible without determination of the local electronic energy density, H_{BCP}. According to Rozas *et al.* [58], the character of interaction could be classified as function of the H_{BCP} with Laplacian of the electron density at BCP ($\nabla^2\rho_{BCP}$). It means that for strong interactions ($\nabla^2\rho_{BCP} < 0$ and $H_{BCP} < 0$) the covalent character is established, for medium strength ($\nabla^2\rho_{BCP} > 0$ and $H_{BCP} < 0$) their partially covalent character is defined, and weak ones ($\nabla^2\rho_{BCP} > 0$ and $H_{BCP} > 0$) are mainly electrostatic. Thus, the magnitude of H_{BCP} indicates the "degree of covalency" present in a given interaction.

Figure 3 clearly shows the existence of a BCP for each F···F, Br···Br and Br···O interaction, accompanied by a bond path between the two corresponding atoms. It can be seen that the calculated values of ρ_{BCP} are in the range of 0.004-0.009 au, whereas the values of $\nabla^2\rho_{BCP}$ are all positive, ranging from 0.023-0.034 au. This indicates very little sharing between the two atomic basins, leading one to anticipate small delocalization between the basins of the two corresponding atoms. We noted, however, the ρ_{BCP} value is

slightly higher for the Br···O bond compared to the Br···Br and F···F interactions. This confirms the idea that the strength of the halogen bond is connected with the anisotropy of the electron charge distribution of X atom (as a Lewis acid) as well as the magnitudes of the $V_{S,min}$ of B (as a Lewis base). The electron density at the F···F critical points compares well to those reported in the literature, for example, H-F···F-F [59], C-F···F-C in difluorinated aromatics [37], or H_3C-H···F-CH_3 [60]. Finally, there does appear to be a correlation between the electron density at F···F critical point and intermolecular bond distances (Fig. 4a). In summary, our computational study reveals that the interactions present in the solid BFNB can be characterized as weak, but stabilizing interactions.

Earlier studies have established that a partly covalent interaction is connected with a positive value for $\nabla^2\rho_{BCP}$ and a negative value for H_{BCP} [58]. An alternative tool for assessing the nature of interaction is the absolute ratio of kinetic energy and potential energy densities, $-G_{BCP}/V_{BCP}$. Accordingly, if $-G_{BCP}/V_{BCP} > 1$ the interaction is noncovalent in nature. On the other hand, if $0.5 < -G_{BCP}/V_{BCP} < 1$ then the interaction is partly covalent. In Table 1, the small values of ρ_{BCP}, the positive values of the $\nabla^2\rho_{BCP}$, $-G_{BCP}/V_{BCP} > 1$ and the nearly zero values of H_{BCP} suggest, according to the Rozas [58] criterion, that the all F···F, Br···Br and Br···O interactions, are weak and basically electrostatic in nature. More specifically, it can be seen that the values of H_{BCP} obtained for the F···F interactions are about 0.010 au, which are slightly smaller than that at the Br···O BCP. This shows that the F···F bond exhibits clear electrostatic character, supporting the main contribution of the electrostatic interaction in this type of halogen bond. Also, the calculated $-G_{BCP}/V_{BCP}$ values in Table 1 are greater than unity for the all the F···F, Br···Br and Br···O interactions considered here, indicating that the kinetic energy overcomes the potential energy density at the BCP. Figure 4b presents the dependencies between the F···F distance and the energetic topological parameters H_{BCP}, V_{BCP}, and G_{BCP}. One can see that the changes of these parameters are monotonic; G_{BCP} increases, V_{BCP} decreases, and H_{BCP} practically does not change if the F···F distance decreases. Further, these results are in good agreement with the reported values in the literature for weak F···F interactions [37].

Interaction Energies and Energy Decomposition Analysis (EDA)

In this section, we study the stabilizing energy between dimeric fragments of BFNB monomers in the solid phase. Table 2 gives the interaction energies of the five BFNB dimers calculated by means of all electron MP2 and M06-2X methods using 6-311++G(d,p) basis set. Some interesting features can be learned from the inspection of the interaction energies. Among all BFNB dimers, No.1···No.4 with one C-Br···O contact of length 3.15 Å as well as one F···F interaction of length 3.01 Å is the most stable dimer. It can be observed that the interaction energy amounts to -5.85 kcal mol^{-1} at the MP2/6-311++G(d,p) level for this dimer. The M06-2X gives rather similar result, though interaction energy is slightly greater. These results are in consistent with the MP2 stabilization energies for other Br···O interactions [8]. The stabilization energy gained for each F···F interaction in dimer No.1···No.2 is approximately -1.8 kcal mol^{-1}. The contribution of each F···F contact to the total interaction energy of the other dimers is also noticeable, however it is comparable to other theoretical studies present in the literature [33,35]. The computed interaction energies of the dimer No.1···No.3, where only one F···F interaction is formed, are -1.07 kcal mol^{-1} and -2.24 kcal mol^{-1} at the MP2 and M06-2X/6-311++G** levels of theory, respectively. On the other hand, the stabilization caused due to Br···Br formation is almost less significant compared to the Br···O and F···F bonds. This is due to the long Br···Br distances, which are slightly larger than the sum of vdW radii. In a prior study of solid 2,6-dibromo-4-nitroaniline, it was found that analogous Br···Br gives an average interaction energy -2.49 kcal mol^{-1} [61].

To gain more insight about the nature of the interactions, we further performed EDA calculations to analyze the interaction energies in terms of meaningful physical components such as electrostatic, polarization, dispersion, and exchange-repulsion energies [40]. The decomposition of the interaction energies were performed according to Eq. (1) described in Computational details. The results for the dimers analyzed here are given in Table 2. As seen in this table, all contributions of the electrostatic, polarization and dispersion terms have a stabilizing effect. For all dimers studied, the exchange-repulsion energy becomes even larger than the absolute value of the electrostatic energy, but the

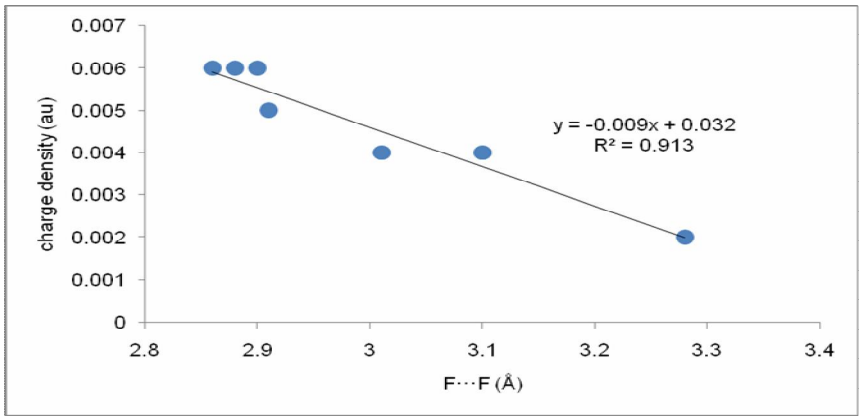

(a)

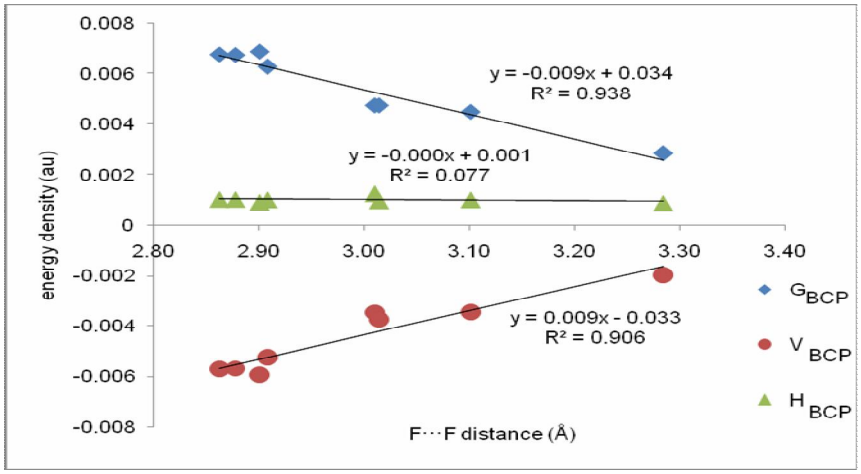

(b)

Fig. 4. Correlation between F···F distances and (a) electron density, (b) different energy density terms at the corresponding BCPs.

Table 1. Intermolecular Distances r, Angles θ, and Calculated (M06-2X/6-311++G**) Electron Density ρ_{BCP}, its Laplacian $\nabla^2\rho_{BCP}$, Total Electronic Density H_{BCP} and the Absolute Ratio of G_{BCP} and V_{BCP} for Crystalline BFNB

Interaction	r(Å)	θ(°)	ρ_{BCP} (au)	$\nabla^2\rho_{BCP}$ (au)	H_{BCP} (au)	$-G_{BCP}/V_{BCP}$
CF1(1)···F2(5)	2.91	169.50	0.005	0.029	0.0010	1.19
CF1(1)···F2(6)	3.01	174.02	0.004	0.024	0.0010	1.25
CF2(1)···F3(2)	2.90	127.88	0.006	0.031	0.0009	1.15
CF2(1)···F4(2)	2.86	176.05	0.006	0.031	0.0010	1.18
CF3(1)···F3(4)	3.01	174.04	0.004	0.023	0.0010	1.26
CF4(1)···F3(3)	2.88	168.68	0.006	0.031	0.0010	1.18
CBr(1)···Br(4)	3.88	147.61	0.005	0.016	0.0009	1.42
CBr(1)···O2(5)	3.15	155.89	0.009	0.033	0.0012	1.20
O2(1)···Br(6)C	3.15	155.89	0.009	0.034	0.0012	1.20

Table 2. Calculated Interaction Energies and EDA Results for Different BFNB Dimers[a]

dimer	E_{int}^{M06-2X}	E_{int}^{MP2}	E_{elst}	$E_{exch-rep}$	E_{pol}	E_{disp}
No. 1-No.2	-4.22	-3.60	-2.71	2.94	-1.95	-1.88
No. 1-No.3	-2.24	-1.97	-1.78	2.24	-1.28	-1.15
No. 1-No.4	-6.55	-5.85	-2.13	3.16	-2.61	-4.27
No. 1-No.5	-4.81	-4.31	-1.90	2.63	-1.93	-3.11
No. 1-No.6	-6.69	-5.58	-2.04	3.05	-2.48	-4.11

[a]All energies and energy terms in kcal mol^{-1}.

Table 3. Calculated NMR Parameters for ^{19}F and ^{79}Br Nuclei of Crystalline BFNB[a,b]

Nuclei	M062X		B3LYP	
	σ_{iso}	$\Delta\sigma$	σ_{iso}	$\Delta\sigma$
F1	298 (306)	131 (159)	298 (301)	125 (143)
F2	310 (324)	185 (194)	310 (318)	181 (165)
F3	303 (306)	138 (159)	302 (301)	132 (143)
F4	318 (324)	179 (194)	317 (318)	171 (165)
Br	2016 (2118)	866 (881)	2032 (2052)	859 (985)

[a]The numbers within the parenthesis are referred to the isolated gas phase monomer. [b]The values out of parenthesis are referred to the crystalline phase.

large attractive polarization and dispersion energies lead to a stabilizing interaction. It is found that for the majority of the F···F, the most stabilizing interaction energy components are electrostatic and polarization. For the No.1···No.4 dimer, the major contribution is the dispersion energy which presents 47% of the total stabilization energy. EDA results also show that the electrostatic effects account for about 42% of the overall attraction in the F···F bonded dimers. By comparison, the polarization component of this interaction represents 28% of the total attractive forces, while dispersion contributes 30% to the stability of these structures. In summary, it can be said that the F···F interactions are remarkably dependent on electrostatic forces. In contrast, the stabilities of the Br···Br and Br···O halogen bonds are predicted to be attributable mainly to dispersion and polarization effects, while electrostatic forces play a smaller role.

NMR Parameters

Listed in Table 3 are DFT results for shielding isotropy(σ_{iso}) and anisotropy ($\Delta\sigma$) parameters at the sites of ^{19}F and ^{79}Br nuclei of BFNB in both gas phase and crystalline lattice. At first glance to the calculated results, some interesting trends can be easily obtained. For those nuclei participated in the intermolecular interactions, NMR parameters exhibit meaningful changes on going from the isolated molecule model to the target molecule in the cluster. Of course, the magnitude of these changes at each nucleus depends directly on its amount of contribution to the interactions. On the other hand, the difference between σ_{iso} and $\Delta\sigma$ for different nuclei of the BFNB in gas-phase and the crystalline lattice is attributed to intermolecular effects, which are known to be predominantly deshielding [62]. Considering the calculated σ_{iso} and $\Delta\sigma$ values of crystalline BFNB with the 6-311++G** basis set, it is evident that the results obtained by M06-2X and B3LYP methods are practically coincident with each other.

Figure 1 indicates that there are four crystallographically distinct fluorine sites in BFNB [44]. As reported in Table 3, all of the $\sigma_{iso}(^{19}F)$ values of the monomer BFNB lie within the 306-324 ppm (with M06-2X method) and those of the

F2 and F4 atoms are relatively more shielded. Clearly, a different σ_{iso} and $\Delta\sigma$ values observed for the fluorine sites in the monomer BFNB must arise from differences in the surrounding environment. A quick look at the results reveals that intermolecular F···F interactions affect the calculated NMR parameters at the fluorine sites; however, such an influence is not equivalent for the four F nuclei. As seen in Table 3, M06-2X/6-311++G** calculations reveal that the $\sigma_{iso}(^{19}F)$ of F2 decreases by 14 ppm depending on whether the BFNB molecule is in the gas phase or in the crystal lattice. On the other hand, the corresponding $\Delta\sigma$ parameter decreases about 9 ppm on going from the single monomer to the target molecule in the cluster. These significant changes reveal the importance of the F···F interactions in contributing to the weak intermolecular interactions in the crystalline BFNB. The σ_{iso} parameter for F2 atom in crystalline BFNB is calculated to be 310 ppm. This value, which is obtained by taking the whole cluster into consideration, is expected to be close to those of fluorinated benzene derivatives [63]. In contrast, the ^{19}F NMR parameters for the remaining F atoms show less sensitivity to the intermolecular interactions. Figure 1 indicates that F1 contributes to the two different F···F interactions in the crystalline BFNB. Due to the such weak F···F interactions, σ_{iso}(F1) is decreased by 8 ppm from the monomer to the target molecule in the cluster. The $\Delta\sigma$ parameter is also decreasesd by 28 ppm from the monomer to the cluster. This is due to the limited involvement of this nucleus in the intermolecular interaction of BFNB in its solid phase.

As noted above, the Br atom of the target molecule contributes to the CBr(1)···Br(4) as well as CBr(1)···O2(5) intermolecular halogen bonding interactions in the crystalline BFNB. For the NMR parameters of this site, the comparison of the isolated model and the hexamer cluster shows discrepancies, more significant than those as the one sees for ^{19}F nuclei. The M06-2X/6-311++G** calculations reveal that σ_{iso} at the site of Br atom is decreased by 98 ppm from the monomer to the target molecule in the cluster. Besides, the corresponding $\Delta\sigma$ value at this site is decreased from 881 ppm (in monomer) to 866 ppm (in cluster).

CONCLUDING REMARKS

In this work, we reporte a systematic computational study on intermolecular interactions in crystalline BFNB by means of quantum chemical calculations. The intermolecular F···F distances of crystalline BFNB are in a range from 2.86 to 3.01 Å. Most of them are less than or in the vicinity of sums of the vdW radii of the respective atoms, which is consistent with these being weak interactions. It can be seen that the values of ρ_{BCP} are calculated to be in a range of 0.004-0.009 au, whereas the values of $\nabla^2\rho_{BCP}$ are all positive, ranging from 0.023-0.034 au. This indicates very little sharing between the two atomic basins, leading one to anticipate small delocalization between the basins of the two corresponding atoms. An acceptable correlation evident between the F···F distances and the electron densities as well as kinetic energy densities at the corresponding BCPs. According to the EDA results, the F···F interactions are remarkably dependent on electrostatic forces. In contrast, the stabilities of the Br···Br and Br···O halogen bonds are predicted to be attributable mainly to dispersion and polarization effects, while electrostatic forces play a smaller role. NMR calculations reveal that the F···F, Br···Br and Br···O intermolecular interactions affect the calculated chemical shielding parameters at the ^{19}F and ^{79}Br sites. This indicates that NMR parameters at the sites of the ^{19}F and ^{79}Br are, as such, appropriate parameters to characterize the properties of these interactions in crystalline BFNB.

REFERENCES

[1] S. Scheiner, Hydrogen Bonding: A Theoretical Prospective; Oxford University Press, Oxford, UK, 1997.

[2] H.K. Woo, X.B. Wang, L.S. Wang, K.C. Lu, J. Phys. Chem. A 109 (2005) 10633.

[3] P. Hobza, Z. Havlas, Chem. Rev. 100 (2000) 4253.

[4] J. Thar, B. Kirchner, J. Phys. Chem. A 110 (2006) 4229.

[5] C. Guardigli, R. Liantonio, M.L. Mele, P. Metrangolo, G. Resnati, T. Pilati, Supramol. Chem. 15 (2003) 177.

[6] G.R. Desiraju, T. Steiner, The Weak Hydrogen Bond, Oxford University Press, Oxford, UK, 1999.

[7] P. Politzer, J.S. Murray, M.C. Concha, J. Mol. Model. 13 (2007) 643.

[8] K.E. Riley, J.S. Murray, P. Politzer, M.C. Concha, P. Hobza, J. Chem. Theory Comput. 5 (2009) 155.

[9] P. Metrangolo, Y. Carcenac, M. Lahtinen, T. Pilati, K. Rissanen, A. Vij, G. Resnati Science 323 (2009) 1461.
[10] K. Riley, P. Hobza, J. Chem. Theory Comput. 4 (2008) 232.
[11] C.B. Aakeröy, M. Fasulo, N. Schultheiss, J. Desper, C. Moore, J. Am. Chem. Soc. 129 (2007) 13772.
[12] M.D. Esrafili, J. Mol. Model. 18 (2012) 5005.
[13] Z.P. Shields, J.S. Murray, P. Politzer, Int. J. Quantum Chem. 110 (2010) 2823.
[14] E. Corradi, S.V. Meille, M.T. Messina, P. Metrangolo, G. Resnati, Angew. Chem. Int. Ed. 39 (2000) 1782.
[15] T. Brinck, J.S. Murray, P. Politzer, Int. J. Quantum Chem. 44 (1992) 57.
[16] T. Clark, M. Hennemann, J.S. Murray, P. Politzer, J. Mol. Model. 13 (2007) 291.
[17] P. Murray-Rust, W.D.S. Motherwell, J. Am. Chem. Soc. 101 (1979) 4374.
[18] S. Triguero, R. Llusar, V. Polo, M. Fourmigué, Cryst. Growth Des. 6 (2008) 2241.
[19] K. Raatikainen, K. Rissanen, Cryst. Eng. Commun. 13 (2011) 6972.
[20] P. Politzer, J.S. Murray, M.C. Concha, J. Mol. Model. 14 (2008) 659.
[21] G. Trogdon, J.S. Murray, M.C. Concha, P. Politzer, J. Mol. Model. 13 (2007) 313.
[22] F.F. Awwadi, R.D. Willett, K.A. Peterson, B. Twamley, Chem. Eur. J. 12 (2006) 8952.
[23] M.D. Esrafili, B. Ahmadi, Comput. Theor. Chem. 997 (2012) 77.
[24] M.D. Esrafili, M. Solimannejad, J. Mol. Model. (in press) DOI 10.1007/s00894-013-1912-y.
[25] P. Politzer, J.S. Murray, T. Clark, Phys. Chem. Chem. Phys. (in press) DOI: 10.1039/c3cp00054k.
[26] P. Politzer, J.S. Murray Chem. Phys. Chem. 14 (2013) 278.
[27] T.S. Thakur, M.T. Kirchner, D. Blaser, R. Boese, G. Desiraju, Cryst. Eng. Comm. 12 (2010) 2079.
[28] G. Cavallo, P. Metrangolo, T. Pilati, G. Resnati, M. Sansotera, G. Terraneo, Chem. Soc. Rev. 39 (2010) 3772.
[29] T.T.T. Bui, S. Dahaoui, C. Lecomte, G.R. Desiraju, E. Espinosa, Angew. Chem. Int. Ed. 48 (2009) 3838.
[30] B.K. Saha, R.K.R. Jetti, L.S. Reddy, S. Aitipamula, A. Nangia, Cryst. Growth Des. 5 (2005) 887.
[31] N. Ramasubbu, R. Parthasarathy, P. Murray-Rust, J. Am. Chem. Soc. 108 (1986) 4308.
[32] V. Tsirelson, P.F. Zou, T.-H. Tang, R.F.W. Bader, Acta Crystallogr. Sect. A 51 (1995) 143.
[33] M. Barceló-Oliver, C. Estarellas, A. García-Raso, A. Terrón, A. Frontera, D. Quiñonero, I. Mata, E. Molins, P.M. Deyà, Cryst. Eng. Comm. 12 (2010) 3758.
[34] P. Zhou, J. Zou, F. Tian, Z. Shang, J. Chem. Inf. Model. 49 (2009) 2344.
[35] R.J. Baker, P.E. Colavita, D.M. Murphy, J.A. Platts, J.D. Wallis, J. Phys. Chem. A 116 (2012) 1435.
[36] A. Bach, D. Lentz, P. Luger, J. Phys. Chem. A 105 (2001) 7405.
[37] C.F. Matta, N. Castillo, R.J. Boyd, J. Phys. Chem. A 109 (2005) 3669.
[38] I. Alkorta, J. Elguero, Struct. Chem. 15 (2004) 117.
[39] R.F.W. Bader, Atoms in Molecules-a Quantum Theory, Oxford University Press, New York, 1990.
[40] M.W. Schmidt, K.K. Baldridge, J.A. Boatz, S.T. Elbert, M.S. Gordon, J.H. Jensen, S. Koseki, N. Matsunaga, K.A. Nguyen, S.J. Su, T.L. Windus, M. Dupuis, J.A. Montgomery, J. Comput. Chem. 14 (1993) 1347.
[41] A.D. Becke, J. Chem. Phys. 98 (1993) 5648.
[42] Y. Zhao, D.G. Truhlar, Theor. Chem. Acc. 120 (2008) 215.
[43] Y. Zhao, D.G. Truhlar, J. Chem. Phys. 125 (2006) 194101.
[44] M. Stein, A. Schwarzer, J. Hulliger, E. Weber, Acta Crystallogr. Sec. E 67 (2011) 1655.
[45] S.F. Boys, F. Bernardi, Mol. Phys. 19 (1970) 553.
[46] P. Su, H. Li, J. Chem. Phys. 131 (2009) 014102.
[47] K. Wolinski, J.F. Hilton, P. Pulay, J. Am. Chem. Soc. 112 (1990) 8251.
[48] F. Biegler-Konig, J. Schonbohm, D. Bayles, J. Comput. Chem. 22 (2001) 545.
[49] F.A. Bulat, A. Toro-Labbe, T. Brinck, J.S. Murray, P. Politzer, J. Mol. Model. 16 (2010) 1679.
[50] P. Metrangolo, J.S. Murray, T. Pilati, P. Politzer, G. Resnati, Cryst. Eng. Comm. 13 (2011) 6593.
[51] A. Bondi, J. Phys. Chem. 68 (1964) 441.
[52] P. Metrangolo, J.S. Murray, T. Pilati, P. Politzer, G. Resnati, G. Terraneo, Cryst. Growth Des. 11 (2011) 4238.
[53] M. Solimannejad, M. Malekani, I. Alkorta, J. Mol.

Struct. (THEOCHEM) 955 (2010) 140.
[54] P. Lipkowski, S.J. Grabowski, J. Leszczynski, J. Phys. Chem. A 110 (2006) 10296.
[55] M.D. Esrafili, N.L. Hadipour, Mol. Phys. 109 (2011) 2451.
[56] S.J. Grabowski, J. Phys. Chem. A 116 (2012) 1838.
[57] Y.X. Lu, J.W. Zou, Y.H. Wang, Y.J. Jiang, Q.S. Yu, J. Phys. Chem. A 111 (2007) 1078.
[58] I. Rozas, I. Alkorta, J. Elguero, J. Am. Chem. Soc. 122 (2000) 11154.
[59] I. Alkorta, I. Rozaz, J. Elguero, J. Phys. Chem. A 102 (1998) 9278.
[60] E. D'Oria, J.J. Novoa, Cryst. Eng. Comm. 10 (2008) 423.
[61] M.D. Esrafili, J. Mol. Model. 19 (2013)1417.
[62] R. Ida, M. De Clerk, G. Wu, J. Phys. Chem. A 110 (2006) 1065.
[63] G.A. Webb, P.B. Kardakov, J.A. England, Bull. Pol. Acad. Sci. Chem. 48 (2000) 101.